

Language-Driven Visual Consensus for Zero-Shot Semantic Segmentation

Zicheng Zhang¹ Tong Zhang⁴ Yi Zhu² Jianzhuang Liu²
 Xiaodan Liang³ QiXiang Ye⁵ Wei Ke¹

¹School of Software Engineering, Xi'an Jiaotong University

²Huawei Noah's Ark Lab ³Sun Yat-sen University ⁴EPFL

⁵University of Chinese Academy of Sciences

Abstract

The pre-trained vision-language model, exemplified by CLIP [50], advances zero-shot semantic segmentation by aligning visual features with class embeddings through a transformer decoder to generate semantic masks. Despite its effectiveness, prevailing methods within this paradigm encounter challenges, including overfitting on seen classes and small fragmentation in masks. To mitigate these issues, we propose a Language-Driven Visual Consensus (LDVC) approach, fostering improved alignment of semantic and visual information. Specifically, we leverage class embeddings as anchors due to their discrete and abstract nature, steering vision features toward class embeddings. Moreover, to circumvent noisy alignments from the vision part due to its redundant nature, we introduce route attention into self-attention for finding visual consensus, thereby enhancing semantic consistency within the same object. Equipped with a vision-language prompting strategy, our approach significantly boosts the generalization capacity of segmentation models for unseen classes. Experimental results underscore the effectiveness of our approach, showcasing mIoU gains of 4.5% on the PASCAL VOC 2012 and 3.6% on the COCO-Stuff 164k for unseen classes compared with the state-of-the-art methods.

1. Introduction

The past decade has witnessed the tremendous success of deep learning methods [8, 9, 35, 51, 56, 63, 65] in the field of semantic segmentation. However, limited to labor-intensive pixel-wise annotations, it is difficult to extend these methods to scenarios with a greater number of object categories. This hinders their application in open-world scenarios, such as autonomous driving [27, 29] and embodied intelligence [23, 55]. To overcome this problem, Zero-Shot Semantic Segmentation (ZS3) [3] is proposed to extend the capability of aligning pixels with pre-defined

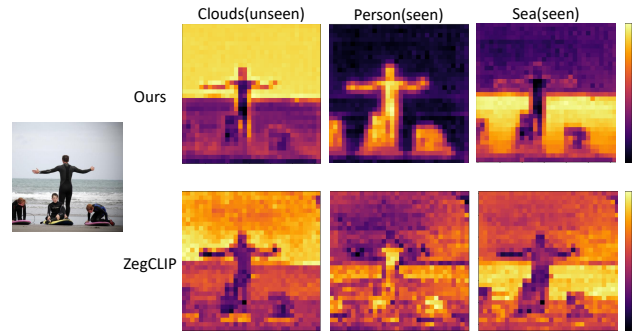


Figure 1. We visualize the cross attention maps between image features and class embeddings from last transformer decoder block in both our approach and the SOTA method, *i.e.*, ZegCLIP [69]. It shows that our approach establishes a clearer, more explicit alignment between dense image features and class embeddings.

classes to novel unseen classes.

Recently, the emergence of vision-language pre-trained models [12, 30, 41, 50, 60] boost the development of ZS3 due to their remarkable image-level zero-shot capability. Consequently, the primary challenge in ZS3 has transitioned to transferring this zero-shot capability from the image level to the pixel level. Pioneering works [15, 49, 62] initially introduced a two-stage method, employing a mask proposal network for mask generation and CLIP as an open-vocabulary classifier for mask labeling. Subsequent endeavors [34, 38, 52, 66, 69] propose a one-stage method to enhance inference speed while maintaining or improving segmentation performance. It equips CLIP model with an extra decoder for further tuning alignment in pixel level. Among those works, ZegCLIP [69] underscores the importance of fine-tuning strategies. Compared to full fine-tuning and parameter-free tuning, parameter-efficient tuning can achieve a trade-off between maintaining zero-shot ability from CLIP and better segmentation performance.

Despite these advancements, the one-stage method still encounters with overfitting on seen classes [39], attributed to the lack of appropriate modifications in the transformer

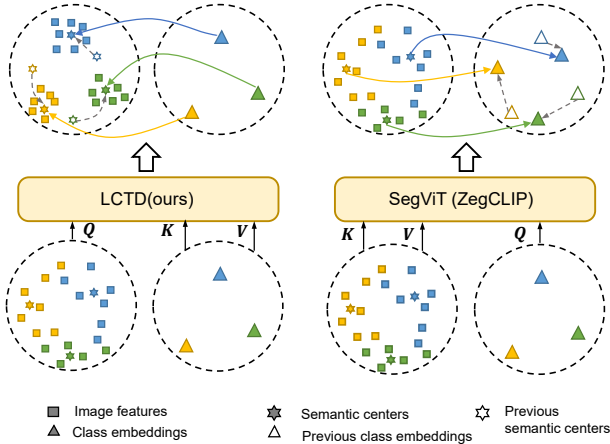


Figure 2. **Illustration of difference between Our Decoder and ZegCLIP’s Decoder [69].** We depict the change of the visual and semantic spaces before and after the decoder. Our approach initially contracts the region of the visual space, maximizing its similarity to the class embeddings. In contrast, ZegCLIP [69] pushes class embeddings towards noisy and redundant visual cues, resulting in significant semantic drift.

decoder [6], such as SegViT [63]. This line of works commonly selects class embeddings from CLIP’s text encoder as query and image features as key and value in cross attention. While effective in fully supervised semantic segmentation, this paradigm falters in zero-shot semantic segmentation, especially when introducing novel classes during inference. This stems from the fact that the visual space from CLIP is not structured enough for segmentation [66]. Moreover, parameter-free/efficient fine-tuning introduces constraints on updates. Considering the redundant nature of visual cues, pushing class embeddings toward visual features can dramatically shift the existing semantic space, compromising zero-shot ability, as depicted in Fig. 2. In contrast, language is a more abstract and highly structured concept, especially in the context of fine-tuning on the CLIP model. This inherent richness in linguistic representation enables the model to capture diverse visual information encapsulated by language. Consequently, making subtle adjustments to the semantic space facilitates the model’s adaptability to new datasets while preserving the robust generalization ability inherited from CLIP.

Building upon this intuition, we present our Language-Driven Visual Consensus (LDVC) approach, designed to perform comprehensive fine-tuning on both visual and language prompts. In this approach, we utilize language representations as anchors to guide the refinement of visual cues. Specifically, we implement a straightforward substitution where image features act as query, and class embeddings serve as both key and value in the cross-attention mechanism of the transformer decoder. This substitution serves a dual purpose: it ensures the consistency of class embed-

dings and contributes to the creation of a more compact visual space. Additionally, we introduce a Local Consensus Transformer Decoder (LCTD) to function as the pixel alignment decoder, updating image features under the guidance of class embeddings. To address noise introduced by the redundancy in visual cues, we apply a route attention mechanism, effectively alleviating small fragmentation in segmentation masks before their alignment with class embeddings. The compactness of the visual space not only enhances the alignment process but also facilitates effective language tuning, as depicted in Fig. 2. This strategic adjustment serves to mitigate the risk of semantic drift and promotes the development of a more stable and structured semantic space during fine-tuning. Consequently, this fortifies the zero-shot capability of the model, making it more resilient and adaptable across diverse datasets.

In a nutshell, our contributions can be summarized as:

- A new local consensus transformer decoder is proposed to alleviate overfitting on unseen classes and reduce the small fragmentation in masks.
- A vision-language prompt tuning strategy is proposed to generalize the pre-trained CLIP to zero-shot semantic segmentation, which further improves unseen classes segmentation ability.

To validate the effectiveness of our approach, we conduct experiments on the publicly available PASCAL VOC 2012 and COCO-Stuff 164k datasets. Results demonstrate that our approach outperforms the state-of-the-art method by 0.6% for seen classes and 4.5% for unseen classes on the PASCAL VOC 2012 dataset, as well as 3.0% and 3.6% on the COCO-Stuff 164k dataset, respectively.

2. Related Works

Zero-Shot Semantic Segmentation. Despite the significant success of deep learning methods [8, 9, 35, 51, 56, 63, 65] in image segmentation, the difficulty in obtaining pixel-wise annotations has constrained the generalization of these approaches. To overcome this problem, researchers propose zero-shot semantic segmentation [3]. Nowadays, depending on the granularity of zero-shot, this task develop two streams. One stream [5, 7, 20, 46, 47, 53, 61] focuses on how to learn region-text alignment during pretraining stage, which eases the demand for pixel-level annotations. The other stream focuses on transferring the alignment capability of image-text pretrained models [12, 30, 41, 50, 60] to the pixel-text level during fine-tuning stage. Recent works in this stream derive two methods: two-stage method and one-stage method. Two-stage method [15, 49, 62] decouples mask generation and mask classification. It first utilizes a mask proposal network to generate class-agnostic masks and then leverages a pretrained image-text model, like CLIP [50] to classify the masked regions in image. Although it well maintains the zero-shot capabilities of CLIP,

the inference cost is heavy due to the separate classification of the huge amount of masked regions per image. The one-stage method [16, 24, 26, 32, 34, 38, 52, 66, 69], however, directly finetunes the pretrained text-image model or distills its knowledge to a side network on segmentation datasets. One-stage method has lower inference costs but sacrifices some degree of alignment capabilities of the pretrained model. Our new local consensus transformer decoder effectively addresses the issue of overfitting on seen classes in one-stage methods.

Prompt tuning. Prompt tuning was first introduced in natural language processing [2, 37, 40]. This technique freezes the parameters of pretrained language model and utilizes additional tokens to facilitate fine-tuning of language models. This new fine-tuning strategy, while adapting to downstream tasks, better avoids “catastrophic forgetting” [21]. Due to its effectiveness, recent works try to introduce this technique into vision language model learning. The approaches in this field can be divided into three aspects: 1) vision-only prompt tuning, 2) language-only prompt tuning, and 3) vision-language prompt tuning.

Vision-only prompt tuning mainly focuses on fine-tuning of pretrained ViT [17]. VPT [31] and EXPRES [14] insert additional learnable tokens between image patch tokens and [CLS] token in each block during fine-tuning. Language-only prompt tuning [45, 52, 67, 68, 70] focuses on optimizing downstream text prompts close to the format of text used for CLIP [50] pretraining. CoOp [68] first introduced learnable prompt tokens in text embeddings. Further, CoCoOp [67] and DenseCLIP [52] use image features to condition learnable prompt tokens for better adaption. Vision-language prompt tuning [33, 36] inserts learnable prompt tokens in both the visual encoder and the text encoder for CLIP’s fine-tuning. We introduces vision-language prompt tuning into zero-shot semantic segmentation task and demonstrates it expands the zero-shot segmentation capability of CLIP.

3. Methodology

In this section, we first provide a brief introduction to the ZS3 setting and review a meta-architecture for the text-image segmentation model. Then the vision-language prompt tuning for CLIP and the new local-consensus transformer decoder are detailed, which are the keys to maintaining and transferring the alignment of CLIP in ZS3.

3.1. Preliminary

We follow the generalized zero-shot semantic segmentation(GZS3) protocol [59], in which it divides the class set of segmentation datasets into two disjoint subsets: the seen class set C^s and the unseen class set C^u . The model training is conducted only on C^s while evaluation on both C^s and C^u . Specifically, during the training phase, we only have

pixel-wise annotations about C^s on each image. During the inference phase, we need to classify each pixel of the image as one of the classes in $C = C^u \cup C^s$. There are two typical settings for ZS3. Inductive ZS3 setting aims to solve the case that unseen class names are not known during training, while transductive ZS3 setting is specified with the unseen class names. Our method mainly focuses on inductive setting, and we also evaluate the performance of transductive setting.

3.2. Overview Pipeline

Previous works [52, 64, 66, 69] that apply text-image models as backbone to segmentation tasks can be reduced to a simple meta-architecture. This architecture simply casts ZS3 as a pixel-level zero-shot classification problem. This architecture usually consists of three components. CLIP’s image encoder and text encoder extracts dense image features and class embeddings respectively. A pixel alignment decoder aligns class embeddings with dense image features. Finally, a simple dot product between updated class embeddings and updated dense image features produces the segmentation mask logits. For this architecture in ZS3 task, the key lies in maintaining the alignment capability of CLIP and transferring this alignment ability to the pixel level. These two aspects correspond to the fine-tuning strategy for CLIP’s encoders and the approach of alignment in pixel-alignment decoder, respectively.

3.3. Vision-language Prompt Tuning

Based on the meta architecture mentioned above, we first address the fine-tuning approach for CLIP’s encoders. Currently, the approaches for fine-tuning CLIP’s encoders can be divide into three aspects. Full fine-tuning methods update all parameters of CLIP. Parameter-free tuning methods freeze all parameters of CLIP and Parameter-efficient tuning methods [19, 28, 68] update small part of parameters in CLIP. As mentioned in ZegCLIP [69], full fine-tuning methods gain high IoU on seen classes but fail on unseen classes and parameter-free tuning methods fail on seen classes. That means the former undermines CLIP’s alignment capability, while the latter cannot enhance CLIP’s segmentation capability. Thus, parameter-efficient tuning methods become a trade-off solution in this dilemma.

Beyond ZegCLIP, we apply deep prompt tuning [31] on both image and text encoders which shows better performance in Tab. 5. As we choose CLIP ViT-B as our default encoders, both of them are transformer-like [58] networks which process sequence input. Formally, we divide the sequence embeddings e_i in each layer into three parts: prompt embeddings $e_p^{(i)}$, content embeddings $e_c^{(i)}$, global embeddings $e_g^{(i)}$,

$$e^{(i)} = [e_p^{(i)}; e_c^{(i)}; e_g^{(i)}], \tag{1}$$

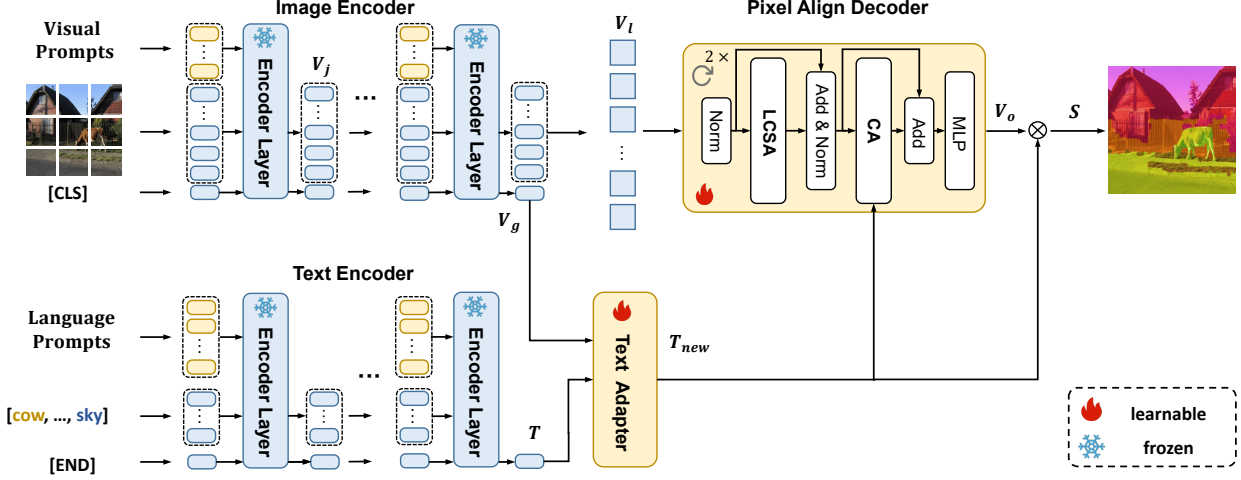


Figure 3. **The architecture of the proposed Language Driven Visual Consensus (LDVC) approach.** We freeze the parameters of CLIP and insert deep learnable visual-language prompts into encoders. Then a text adapter fuses class embeddings T and global image feature V_g . At last, the local-consensus transformer decoder progressively updates the dense visual features V_l under the guidance of updated class embeddings T_{new} to get the final segmentation logits S .

where “[;]” represents concatenation operation of tensor. $e_p^{(i)}$ is deep learnable prompt embeddings in each layer. For vision encoder, $e_c^{(i)}$ corresponds to image patch embeddings and $e_g^{(i)}$ corresponds to [CLS] token embeddings which represent the whole image. For text encoder, $e_c^{(i)}$ corresponds to class name embeddings and $e_g^{(i)}$ corresponds to [EOS] token embeddings which represent the whole sentence. For transformer encoder with l layers, the forward of sequence with learnable prompts can be formulated as:

$$[-; e_c^{(i)}; e_g^{(i)}] = \mathbf{L}_i([e_p^{(i-1)}; e_c^{(i-1)}; e_g^{(i-1)}]), \quad (2)$$

where \mathbf{L}_i denotes i -th layer of transformer. During the training stage, we freeze all parameters in \mathbf{L}_i and only optimize $e_p^{(i)}$.

Through our experiments, we also find that the initialization of $e_p^{(i)}$ has a significant impact on the text encoder. Usually, $e_p^{(i)}$ is initialized from a certain distribution, like uniform or normal distribution. However, we find that the embeddings of hand-crafted prompts would be a better initialization for $e_p^{(i)}$. Specifically, for the input text like “a photo of a {class name}”, we call the template “a photo of a ” as hand-crafted prompts. We first sent these hand-crafted prompts to the pretrained text encoder and extract the corresponding content embeddings $\mathcal{P}^{(i)}$ in each layer. Then we use $\mathcal{P}^{(i)}$ to initialize $e_p^{(i)}$ at the beginning of training. For the prompt embeddings in image encoder, we follow the random initialization as the same as VPT [31].

3.4. Local Consensus Transformer Decoder

After determining the fine-tuning approach for CLIP, we review the design of the pixel alignment decoder. In ZegCLIP, it simply adopts SegViT [63] as its pixel alignment decoder, which is a transformer decoder with attention-to-mask module. It chooses visual features as key and value and class embeddings as query in cross attention layer. It progressively updates the class embeddings and keeps the image features unchanged during decoding stage. As illustrated in introduction, this is suboptimal under parameter-efficient tuning, leading to a less structured visual space. Thus we propose a new local consensus transformer decoder to mitigate this issue.

Specifically, Given an image $I \in \mathbb{R}^{H \times W \times 3}$ and class sets C , the CLIP encoders with visual-language prompts output dense image feature $V_l \in \mathbb{R}^{h \times w \times d}$, multi-intermediate image features $\{V_j\}_{j=1,2,\dots,N}$, global image feature $V_g \in \mathbb{R}^d$ (corresponding to [CLS] token), and class embeddings $T \in \mathbb{R}^{c \times d}$, where h and w are the height and width of dense image features respectively, d is the dimension of the CLIP’s joint embedding space, c is the number of semantic categories, and N is the number of intermediate image features which is equal to the number of blocks in local consensus transformer decoder.

Following the design of previous methods [34, 69], we utilize a text adapter to fuse V_g and T to update class embeddings based on visual cues. The text adapter is implemented as:

$$T_{new} = \mathbf{Proj}([T \odot V_g; T]), \quad (3)$$

where \mathbf{Proj} is a linear projection, \odot represents broadcast

element-wise multiplication. The fused class embeddings $T_{\text{new}} \in \mathbb{R}^{c \times d}$ have the same size as T .

The local consensus transformer decoder chooses image features as query and fused class embeddings T_{new} as key and value in cross-attention. Each block in our decoder consists of local consensus self-attention, cross-attention and multi-layer perception. Formally, the block can be expressed as:

$$V = V_{in} + \mathbf{Conv}(V_j) \quad (4)$$

$$V = V + \mathbf{LCSA}(\mathbf{Norm}(V)) \quad (5)$$

$$V = V + \mathbf{CA}(\mathbf{Norm}(V), \mathbf{Norm}(T_{\text{new}})) \quad (6)$$

$$V_{out} = V + \mathbf{MLP}(\mathbf{Norm}(V)), \quad (7)$$

where V_{in} is the previous block’s output feature and V_j is the the intermediate image feature of CLIP encoder, \mathbf{Conv} is a convolution layer with 1×1 kernel, \mathbf{LCSA} is local consensus self-attention, \mathbf{Norm} is layer normalization [1], \mathbf{CA} represents cross-attention and \mathbf{MLP} is a simple multi-layer perception.

As semantic segmentation can be viewed as a clustering problem, semantic correspondence in objects is crucial in segmentation decoding stage, which can alleviate the phenomenon of small fragmentation in segmentation mask. To better enhance the semantic correspondence in our decoder, our local consensus self-attention utilizes route attention [10, 54, 71] to dynamically select the regions that most semantic-relevant to attend in self-attention layers of the transformer decoder. Specifically, For dense image features V , we first employ an average pooling layer with a window size of $n \times n$ to extract window features $V_w \in \mathbb{R}^{h/n \times w/n \times d}$. Then we calculate the similarity between each window feature and choose m windows that are most semantic-relevant for each window feature. Based on the routing, we constrain self-attention for V in the selected m windows. The operations are as follows:

$$V_w = \mathbf{AvgPool}(V_{in}) \quad (8)$$

$$Q, K, V = \mathbf{Chunk}(\mathbf{Proj}(V_{in})) \quad (9)$$

$$\text{ids} = \mathbf{Topk}(V_w V_w^T, m) \quad (10)$$

$$K_s, V_s = \mathbf{Gather}(K, \text{ids}), \mathbf{Gather}(V, \text{ids}) \quad (11)$$

$$O = \mathbf{Softmax}(Q K_s^T / \sqrt{d}) V_s, \quad (12)$$

where $\mathbf{AvgPool}$ denotes average pooling operation, \mathbf{Proj} denotes linear projection which projects V_{in} from length d to $3d$, \mathbf{Chunk} means splitting the tensor along the last dimension, \mathbf{Topk} returns the indices of m -largest elements of given tensor, \mathbf{Gather} denotes the operation that gathers tensors according to indices, and $\mathbf{Softmax}$ denotes a softmax layer.

Finally, after forwarding several stacked decoder blocks, we get the final image feature $V_o \in \mathbb{R}^{h \times w \times d}$ and we multiply V_o with T_{new} to produce segmentation logits $S \in$

$\mathbb{R}^{c \times h \times w}$, as:

$$S = T_{\text{new}} V_o^T. \quad (13)$$

4. Experiment

4.1. Setting

Datasets. We evaluate our proposed method on two widely used datasets: VOC2012 [18] and COCO-Stuff 164K [4]. VOC2012 contains 10,582 augmented images for training and 1,449 for validation. Following previous works [15, 69], we delete "background" class and use 15 classes as seen classes and 5 classes as unseen classes. COCO-Stuff 164K includes all 164K images from COCO [42], has 171 named categories and contains 118K images for training, 5K for evaluation. We use 156 classes as seen classes and 15 classes as unseen classes. The unseen classes of each dataset are shown in supplementary.

Metrics. Following previous methods, we use three metrics to evaluate our results: mIoU(S), mIoU(U) and hIoU. mIoU(S) and mIoU(U) represent the mean Intersection over Union (mIoU) on seen classes and unseen classes, respectively. hIoU denotes the harmonic mean value of mIoU on seen and unseen classes:

$$hIoU = \frac{2 \times mIoU(S) \times mIoU(U)}{mIoU(S) + mIoU(U)}.$$

Implementation Details. We implement our method based on the MMSegmentation [13] framework. We choose CLIP ViT-B as our default vision and language backbones. The number of visual deep prompt tokens is set as 100 and 40 in each layer of CLIP for COCO-stuff 164k and VOC2012. The number of language deep prompt tokens is 6 in each layer on both datasets. The number of our decoder block is 2. For local consensus self-attention, window size n is 4×4 total number of windows is 64 and the number of selected windows m is 16. Following ZegCLIP, we linearly combine focal loss [43] and dice loss [57] as our training loss. The loss weights for focal loss and dice loss are 100.0 and 1.0, respectively. We crop each image into 512×512 in both the training and evaluation stage. During training, we adopt AdamW [44] as our optimizer and set the initial learning rate as $2e-4$. We use the polynomial learning rate scheduler. The number of iterations for COCO-Stuff 164k and VOC2012 is set as 80k and 20k, respectively. All experiments are conducted on 4 RTX3090 GPUs with the batch size of 16.

4.2. Comparison with State-of-the-Arts

To demonstrate the effectiveness of our method, we compare with previous the-state-of-art methods in Tab. 1 and also provide visualization results on the COCO-Stuff 164k dataset in Fig. 4. Both of them show the great generalization ability on unseen classes of our method.

	Pipeline	PASCAL VOC 2012				COCO-Stuff 164k			
		pAcc	mIoU(S)	mIoU(U)	hIoU	pAcc	mIoU(S)	mIoU(U)	hIoU
SPNet [59]	One-Stage	-	78.0	15.6	26.1	-	35.2	8.7	14.0
ZS3 [3]	One-Stage	-	77.3	17.7	28.7	-	34.7	9.5	15.0
CaGNet [22]	One-Stage	80.7	78.4	26.6	39.7	56.6	33.5	12.2	18.2
SIGN [11]	One-Stage	-	75.4	28.9	41.7	-	32.3	15.5	20.9
STRICT [48]	One-Stage	-	82.7	35.6	49.8	-	35.3	30.3	32.6
ZegFormer [15]	Two-Stage	-	86.4	63.6	73.3	-	36.6	33.2	34.8
Zsseg [62]	Two-Stage	90.0	83.5	72.5	77.5	60.3	39.3	36.3	37.8
DeOP [25]	One-Stage	-	88.2	74.6	80.8	-	38.0	38.4	38.2
ZegCLIP [69]	One-Stage	94.6	91.9	77.8	84.3	62.0	40.2	41.4	40.8
LDVC (Ours)	One-Stage	95.5	92.5	82.3	87.2	64.3	43.2	45.0	44.1

Table 1. Comparison with SOTA methods under "inductive" GZS3 setting on VOC 2012 and COCO-Stuff 164k datasets.

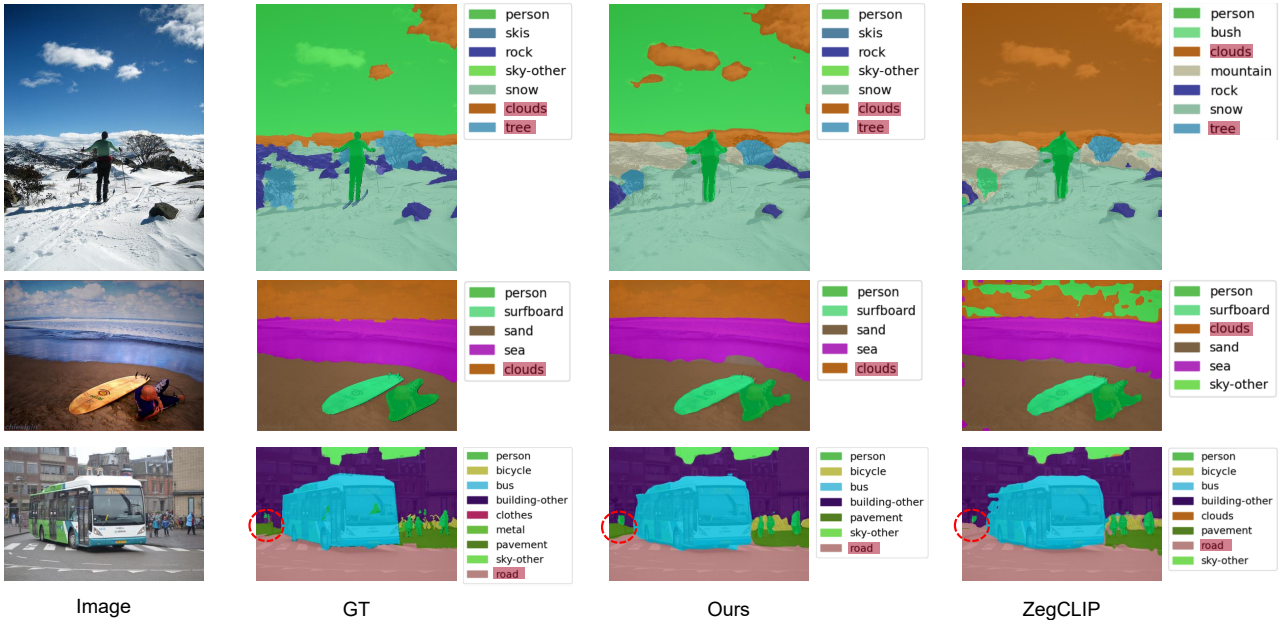


Figure 4. Visualization of segmentation prediction under inductive settings on COCO-Stuff 164k. We compare the segmentation results between our approach and the SOTA method. The categories with color marked are unseen classes and others are seen classes.

Inductive Settings. First, we evaluate our method under inductive settings where the unseen class names are not known during training stage. From Tab. 1, our method surpasses previous approaches on both VOC 2012 and COCO-Stuff 164k datasets. It outperforms DeOP [25] by 7.7% and 6.4% in mIoU(U) and hIoU on VOC 2012, and by 6.6% and 5.9% on COCO-Stuff 164k, respectively. Furthermore, our method exceeds the leading one-stage method ZegCLIP [69] by 4.5% and 2.9% in mIoU(U) and hIoU on VOC 2012, and by 3.6% and 3.3% on COCO-Stuff 164k.

Visualization Results. From Fig. 4, we visualize some segmentation results from our method and the SOTA method on COCO-Stuff 164k validation dataset which contains more objects in a scene. The categories marked with red are

unseen classes. From Fig. 4, we can see that comparing with ZegCLIP, our method recognizes objects in the images more accurately and achieves a higher match with the ground truth classes. In addition, our method is more accurate in predicting unseen class masks, for example, as the red circled part in the bottom row of Fig. 4 shown, our method successfully distinguishes between “road” and “pavement”, while ZegCLIP regards “pavement” as “road”. And on the top of Fig. 4, it illustrates that ZegCLIP segments the whole upper region of the image as the “clouds” category, while our method produces more fine-grained results that successfully distinguish between “clouds” and “sky-other”, which is even more accurate than the ground truth annotation.

Transductive Settings. We also evaluate our method un-

Method	mIoU(S)	mIoU(U)	hIoU
ZegOT [34]+ST	38.2	59.2	46.4
ZegCLIP [69]+ST	40.6	59.9	48.4
Ours+ST	41.1	60.3	48.8

Table 2. Comparison with SOTA methods under transductive ZS3 setting on COCO Stuff164k dataset. “ST” represents self-training.

Method	Params	mIoU	mIoU(S)	mIoU(U)	hIoU
ZegOT [34]	21M	40.1	38.3	58.7	46.4
ZegCLIP [69]	14M	42.7	40.7	63.2	49.6
Ours	11M	46.4	44.5	65.9	53.1

Table 3. Comparison with SOTA methods under fully supervised semantic segmentation on COCO-Stuff 164k dataset, which serves as the upper bound of ZS3 methods.

der transductive settings where the unseen class names are known during training stage. Thus, besides fine-tuning, this setting involves another self-tuning (ST) stage. We follows the same training strategy previous method [34, 62, 69]. From Tab. 2, we compare our method with ZegOT and ZegCLIP on COCO-Stuff 164k datasets. Our method outperforms ZegOT by 2.9% and 1.1% on mIoU(S) and mIoU(U), respectively. Moreover our method exceeds ZegCLIP by 0.5% and 0.4% on mIoU(S) and mIoU(U), respectively. The results demonstrate that our method also performs well under transductive settings.

Fully supervised. We also provide the results of fully supervised semantic segmentation on COCO-Stuff 164k, which serves as the upper bound of our approach. In Tab. 3, compared to ZegClip with 14M learnable parameters and ZegOT with 21M learnable parameters, our model has fewer parameters, specifically 11M. With less learnable parameters, our model still outperforms ZegOT and ZegCLIP by 5.3% and 3.7% on mIoU, respectively. These results demonstrate that our approach can better enhance the segmentation ability of CLIP’s backbone with less learnable parameters.

4.3. Ablation Study

All ablation experiments are conducted on COCO-Stuff 164k validation dataset.

Effectiveness of VLPT and LCTD. The effectiveness of the Vision-language Prompt Tuning (VLPT) and Local Consensus Transformer Decoder(LCTD) is introduced first for the ablation study, as shown in Table 4. The hIoU is improved from 40.8% to 42.2% when VLPT is used with the baseline ZegCLIP [69].

One main difference between the proposed LCTD decoder and SegViT decoder in ZegCLIP lies in that we choose image features as query and class embeddings as key and value in cross attention of the transformer decoder. As we illustrated in Sec. 1, under the parameter-free tuning

VLPT	LCTD	LCSA	mIoU(S)	mIoU(U)	hIoU
			40.2	41.4	40.8
✓			42.3	41.9	42.2
✓	✓		42.8	44.2	43.5
✓	✓	✓	43.2	45.0	44.1

Table 4. Effectiveness of VLPT, LCTD and LCSA.

Prompt Tuning Method	mIoU(S)	mIoU(U)	hIoU
Language-Only	40.92	39.48	40.19
Vision-Only	42.26	43.10	42.68
Vision-Language	43.20	45.02	44.09

Table 5. Ablation of different prompt tuning on CLIP’s encoders.

Prompt Initialization	mIoU(S)	mIoU(U)	hIoU
Random	43.1	40.5	41.8
Pretrain	43.2	45.0	44.1

Table 6. Ablation of different language prompt initialization strategies.

and visual prompt tuning, the updating of visual space is limited, leading to a less structured visual space. This will increase the difficulty of alignment, thereby affecting the segmentation results. Equipped with LCTD without Local Consensus Self-Attention (LCSA), the mIoU(U) gets a gain of 2.3%. It further increases to 45.0% when LCSA is utilized.

Ablation Studies on VLPT. The ablation studies on VLPT are detailed including prompt-tuning strategies, initialization of the language prompt-tuning, and the lengths of language prompt tokens.

We compare different prompt tuning methods first, as shown in Tab. 5. It illustrates that applying deep prompt tuning on both vision and language backbone simultaneously brings the best performance on both seen and unseen classes. If deep prompt tuning is only applied to the language backbone, the performance will decrease 2.28% and 5.54% on seen and unseen classes, respectively. If deep prompt tuning is only applied to the vision backbone, the performance will decrease 0.94% and 1.92%, respectively. The results also show that prompt tuning on the vision backbone has more effects on segmentation performance.

In Tab. 6, we compare different prompt initialization methods on the language backbone. “Random” means we use random Gaussian distribution to initialize prompts and “pretrain” means we use the initial strategy mentioned in Sec 3.3. From the results, the proposed “pretrain” initialization is better than random initialization, especially prominent in unseen classes, where it achieves 4.5% mIoU gain compared to the random initialization.

We also verify the VLPT used as a plug-in to the baseline, as the first row shown in Table 7. In Table 7, it also ver-

Different ZS3 decoders	Frozen			Visual Prompt-tuning			Vision-Language Prompt Tuning		
	mIoU(S)	mIoU(U)	hIoU	mIoU(S)	mIoU(U)	hIoU	mIoU(S)	mIoU(U)	hIoU
ZegCLIP [69]	32.3	32.5	32.4	40.2	41.4	40.8	42.3	41.9	42.2
LDVC w/o LCSA	38.7	39.5	39.1	41.7	42.8	42.2	42.8	44.2	43.5
LDVC	39.8	41.1	40.4	42.3	43.1	42.7	43.2	45.0	44.1

Table 7. Comparison with different ZS3 decoders under parameter-free fine-tuning and different prompt tuning settings.

TopK	mIoU(S)	mIoU(U)	hIoU
8	43.14	44.87	43.99
16	43.20	45.02	44.09
32	43.20	45.00	44.08
48	42.98	44.34	43.64

Table 8. Ablation of the number of selected windows in local consensus self-attention.

Number of Blocks	mIoU(S)	mIoU(U)	hIoU
2	43.20	45.02	44.09
3	43.06	44.67	43.85
4	44.01	43.26	43.63

Table 9. Ablation of the number of decoder blocks.

ifies the LCTD by column comparison. The performances of mIoU(S), mIoU(U), and hIoU are all increased when the CLIP is frozen, tuned with the visual prompt, or the visual-language prompt.

Ablation Studies on LCTD. Next, we give the ablation studies on LCTD about the number of selected windows in local consensus self-attention and the number of stacked decoder blocks.

In Tab. 9, we evaluate the impact of the number of decoder blocks on ZS3 performance. A lightweight local consensus transformer decoder with two block is already sufficient. The performances are similar between a two-layer decoder and a three-layer decoder. Increasing the number of layers leads to a decrease in mIoU(U). Considering both the number of parameters and performance, we stack two decoder blocks. This choice also results in our approach having fewer learnable parameters compared to ZegCLIP, with a total of 11M learnable parameters.

In our local consensus transformer decoder, we replace vanilla self-attention with local consensus self-attention to enhance the local semantic consensus in the same object. In Fig. 5, we visualize the cross attention map in the last block of our decoder. We observe that after incorporating local consensus self-attention, the noise in the cross-attention map is reduced, and the semantics within the same object become more consistent, which demonstrate the effectiveness of local consensus self-attention. Besides, we give the ablation study about the number of selected windows in local consensus self-attention in Tab. 8. The total number of windows in patch features is 64. In Tab. 8, the re-

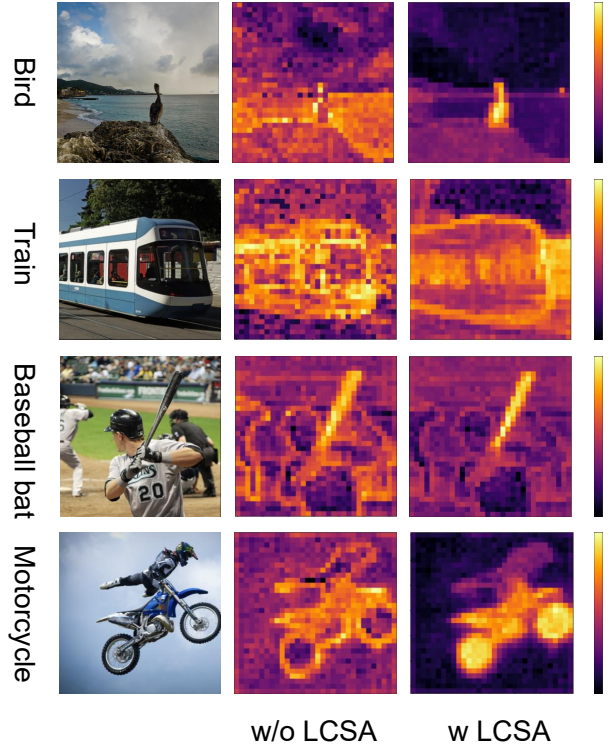


Figure 5. Visualization of cross attention between image features and class embeddings in our decoder with LCSA or without LCSA.

sults show the constant performance when the number is 16 and 32. However, when the number is 48, the local consensus self-attention starts behaving like vanilla self-attention, gathering too many irrelevant patches, leading to a performance decline.

5. Conclusion

We propose a language-driven visual consensus approach for zero-shot semantic segmentation. To solve the issues about overfitting on seen classes and small fragmentation in segmentation masks, we propose a new local consensus transformer decoder which adopts image features as query and class embeddings as key and value in cross attention. To further enhance the semantic consistency of image features in the same object, we introduce route attention mechanism to vanilla self-attention of our decoder. Besides, under a visual-language prompting strategy, our approach further improves segmentation capabilities of CLIP. Exten-

sive experiments have demonstrated the effectiveness of our method. Hope our work can inspire future research.

References

- [1] Jimmy Lei Ba, Jamie Ryan Kiros, and Geoffrey E Hinton. Layer normalization. *arXiv preprint arXiv:1607.06450*, 2016. 5
- [2] Tom Brown, Benjamin Mann, Nick Ryder, Melanie Subbiah, Jared D Kaplan, Prafulla Dhariwal, Arvind Neelakantan, Pranav Shyam, Girish Sastry, Amanda Askell, et al. Language models are few-shot learners. *Advances in neural information processing systems*, 33:1877–1901, 2020. 3
- [3] Maxime Bucher, Tuan-Hung Vu, Matthieu Cord, and Patrick Pérez. Zero-shot semantic segmentation. *Advances in Neural Information Processing Systems*, 32, 2019. 1, 2, 6
- [4] Holger Caesar, Jasper Uijlings, and Vittorio Ferrari. Cocomp: Thing and stuff classes in context. In *Computer vision and pattern recognition (CVPR), 2018 IEEE conference on*. IEEE, 2018. 5
- [5] Kaixin Cai, Pengzhen Ren, Yi Zhu, Hang Xu, Jianzhuang Liu, Changlin Li, Guangrun Wang, and Xiaodan Liang. Mixreorg: Cross-modal mixed patch reorganization is a good mask learner for open-world semantic segmentation. In *Proceedings of the IEEE/CVF International Conference on Computer Vision*, pages 1196–1205, 2023. 2
- [6] Nicolas Carion, Francisco Massa, Gabriel Synnaeve, Nicolas Usunier, Alexander Kirillov, and Sergey Zagoruyko. End-to-end object detection with transformers. In *European conference on computer vision*, pages 213–229. Springer, 2020. 2
- [7] Jun Chen, Deyao Zhu, Guocheng Qian, Bernard Ghanem, Zhicheng Yan, Chenchen Zhu, Fanyi Xiao, Sean Chang Culatana, and Mohamed Elhoseiny. Exploring open-vocabulary semantic segmentation from clip vision encoder distillation only. In *Proceedings of the IEEE/CVF International Conference on Computer Vision*, pages 699–710, 2023. 2
- [8] Bowen Cheng, Alex Schwing, and Alexander Kirillov. Per-pixel classification is not all you need for semantic segmentation. *Advances in Neural Information Processing Systems*, 34:17864–17875, 2021. 1, 2
- [9] Bowen Cheng, Ishan Misra, Alexander G Schwing, Alexander Kirillov, and Rohit Girdhar. Masked-attention mask transformer for universal image segmentation. In *Proceedings of the IEEE/CVF Conference on Computer Vision and Pattern Recognition*, pages 1290–1299, 2022. 1, 2
- [10] De Cheng, Gerong Wang, Bo Wang, Qiang Zhang, Jungong Han, and Dingwen Zhang. Hybrid routing transformer for zero-shot learning. *Pattern Recognition*, 137:109270, 2023. 5
- [11] Jiaxin Cheng, Soumyaroop Nandi, Prem Natarajan, and Wael Abd-Almageed. Sign: Spatial-information incorporated generative network for generalized zero-shot semantic segmentation. In *Proceedings of the IEEE/CVF International Conference on Computer Vision*, pages 9556–9566, 2021. 6
- [12] Mehdi Cherti, Romain Beaumont, Ross Wightman, Mitchell Wortsman, Gabriel Ilharco, Cade Gordon, Christoph Schuhmann, Ludwig Schmidt, and Jenia Jitsev. Reproducible scaling laws for contrastive language-image learning. In *Proceedings of the IEEE/CVF Conference on Computer Vision and Pattern Recognition*, pages 2818–2829, 2023. 1, 2
- [13] MMSegmentation Contributors. MMSegmentation: Openmmlab semantic segmentation toolbox and benchmark. <https://github.com/open-mmlab/mms Segmentation>, 2020. 5
- [14] Rajshekhar Das, Yonatan Dukler, Avinash Ravichandran, and Ashwin Swaminathan. Learning expressive prompting with residuals for vision transformers. *arXiv preprint arXiv:2303.15591*, 2023. 3
- [15] Jian Ding, Nan Xue, Gui-Song Xia, and Dengxin Dai. Decoupling zero-shot semantic segmentation. In *Proceedings of the IEEE/CVF Conference on Computer Vision and Pattern Recognition*, pages 11583–11592, 2022. 1, 2, 5, 6
- [16] Zheng Ding, Jieke Wang, and Zhuowen Tu. Open-vocabulary universal image segmentation with maskclip, 2023. 3
- [17] Alexey Dosovitskiy, Lucas Beyer, Alexander Kolesnikov, Dirk Weissenborn, Xiaohua Zhai, Thomas Unterthiner, Mostafa Dehghani, Matthias Minderer, Georg Heigold, Sylvain Gelly, et al. An image is worth 16x16 words: Transformers for image recognition at scale. *arXiv preprint arXiv:2010.11929*, 2020. 3
- [18] Mark Everingham and John Winn. The pascal visual object classes challenge 2012 (voc2012) development kit. *Pattern Analysis, Statistical Modelling and Computational Learning, Tech. Rep.*, 8(5), 2011. 5
- [19] Peng Gao, Shijie Geng, Renrui Zhang, Teli Ma, Rongyao Fang, Yongfeng Zhang, Hongsheng Li, and Yu Qiao. Clip-adapter: Better vision-language models with feature adapters. *International Journal of Computer Vision*, pages 1–15, 2023. 3
- [20] Golnaz Ghiasi, Xiuye Gu, Yin Cui, and Tsung-Yi Lin. Scaling open-vocabulary image segmentation with image-level labels. In *European Conference on Computer Vision*, pages 540–557. Springer, 2022. 2
- [21] Ian J Goodfellow, Mehdi Mirza, Da Xiao, Aaron Courville, and Yoshua Bengio. An empirical investigation of catastrophic forgetting in gradient-based neural networks. *arXiv preprint arXiv:1312.6211*, 2013. 3
- [22] Zhangxuan Gu, Siyuan Zhou, Li Niu, Zihan Zhao, and Liqing Zhang. Context-aware feature generation for zero-shot semantic segmentation. In *Proceedings of the 28th ACM International Conference on Multimedia*, pages 1921–1929, 2020. 6
- [23] Agrim Gupta, Silvio Savarese, Surya Ganguli, and Li Fei-Fei. Embodied intelligence via learning and evolution. *Nature communications*, 12(1):5721, 2021. 1
- [24] Cong Han, Yujie Zhong, Dengjie Li, Kai Han, and Lin Ma. Open-vocabulary semantic segmentation with decoupled one-pass network. In *Proceedings of the IEEE/CVF International Conference on Computer Vision*, pages 1086–1096, 2023. 3
- [25] Cong Han, Yujie Zhong, Dengjie Li, Kai Han, and Lin Ma. Zero-shot semantic segmentation with decoupled one-pass network. *arXiv preprint arXiv:2304.01198*, 2023. 6

- [26] Kunyang Han, Yong Liu, Jun Hao Liew, Henghui Ding, Jiajun Liu, Yitong Wang, Yansong Tang, Yujiu Yang, Jiashi Feng, Yao Zhao, and Yunchao Wei. Global knowledge calibration for fast open-vocabulary segmentation. In *Proceedings of the IEEE/CVF International Conference on Computer Vision (ICCV)*, pages 797–807, 2023. 3
- [27] Anthony Hu, Lloyd Russell, Hudson Yeo, Zak Murez, George Fedoseev, Alex Kendall, Jamie Shotton, and Gianluca Corrado. Gaia-1: A generative world model for autonomous driving. *arXiv preprint arXiv:2309.17080*, 2023. 1
- [28] Edward J Hu, Yelong Shen, Phillip Wallis, Zeyuan Allen-Zhu, Yuanzhi Li, Shean Wang, Lu Wang, and Weizhu Chen. Lora: Low-rank adaptation of large language models. *arXiv preprint arXiv:2106.09685*, 2021. 3
- [29] Yihan Hu, Jiazhi Yang, Li Chen, Keyu Li, Chonghao Sima, Xizhou Zhu, Siqi Chai, Senyao Du, Tianwei Lin, Wenhui Wang, et al. Planning-oriented autonomous driving. In *Proceedings of the IEEE/CVF Conference on Computer Vision and Pattern Recognition*, pages 17853–17862, 2023. 1
- [30] Chao Jia, Yinfei Yang, Ye Xia, Yi-Ting Chen, Zarana Parekh, Hieu Pham, Quoc Le, Yun-Hsuan Sung, Zhen Li, and Tom Duerig. Scaling up visual and vision-language representation learning with noisy text supervision. In *International Conference on Machine Learning*, pages 4904–4916. PMLR, 2021. 1, 2
- [31] Menglin Jia, Luming Tang, Bor-Chun Chen, Claire Cardie, Serge Belongie, Bharath Hariharan, and Ser-Nam Lim. Visual prompt tuning. In *Computer Vision—ECCV 2022: 17th European Conference, Tel Aviv, Israel, October 23–27, 2022, Proceedings, Part XXXIII*, pages 709–727. Springer, 2022. 3, 4
- [32] Siyu Jiao, Yunchao Wei, Yaowei Wang, Yao Zhao, and Humphrey Shi. Learning mask-aware clip representations for zero-shot segmentation. *arXiv preprint arXiv:2310.00240*, 2023. 3
- [33] Muhammad Uzair Khattak, Hanoona Rasheed, Muhammad Maaz, Salman Khan, and Fahad Shahbaz Khan. Maple: Multi-modal prompt learning. *arXiv preprint arXiv:2210.03117*, 2022. 3
- [34] Kwanyoung Kim, Yujin Oh, and Jong Chul Ye. Zegot: Zero-shot segmentation through optimal transport of text prompts. *arXiv preprint arXiv:2301.12171*, 2023. 1, 3, 4, 7
- [35] Alexander Kirillov, Eric Mintun, Nikhila Ravi, Hanzi Mao, Chloe Rolland, Laura Gustafson, Tete Xiao, Spencer Whitehead, Alexander C Berg, Wan-Yen Lo, et al. Segment anything. *arXiv preprint arXiv:2304.02643*, 2023. 1, 2
- [36] Dongjun Lee, Seokwon Song, Jihee Suh, Joonmyeong Choi, Sanghyeok Lee, and Hyunwoo J Kim. Read-only prompt optimization for vision-language few-shot learning. In *Proceedings of the IEEE/CVF International Conference on Computer Vision*, pages 1401–1411, 2023. 3
- [37] Brian Lester, Rami Al-Rfou, and Noah Constant. The power of scale for parameter-efficient prompt tuning. *arXiv preprint arXiv:2104.08691*, 2021. 3
- [38] Boyi Li, Kilian Q Weinberger, Serge Belongie, Vladlen Koltun, and Rene Ranftl. Language-driven semantic segmentation. In *International Conference on Learning Representations*, 2022. 1, 3
- [39] Jingyao Li, Pengguang Chen, Shengju Qian, and Jiaya Jia. Tagclip: Improving discrimination ability of open-vocabulary semantic segmentation. *arXiv preprint arXiv:2304.07547*, 2023. 1
- [40] Xiang Lisa Li and Percy Liang. Prefix-tuning: Optimizing continuous prompts for generation. *arXiv preprint arXiv:2101.00190*, 2021. 3
- [41] Yanghao Li, Haoqi Fan, Ronghang Hu, Christoph Feichtenhofer, and Kaiming He. Scaling language-image pre-training via masking. In *Proceedings of the IEEE/CVF Conference on Computer Vision and Pattern Recognition*, pages 23390–23400, 2023. 1, 2
- [42] Tsung-Yi Lin, Michael Maire, Serge Belongie, James Hays, Pietro Perona, Deva Ramanan, Piotr Dollár, and C Lawrence Zitnick. Microsoft coco: Common objects in context. In *Computer Vision—ECCV 2014: 13th European Conference, Zurich, Switzerland, September 6–12, 2014, Proceedings, Part V 13*, pages 740–755. Springer, 2014. 5
- [43] Tsung-Yi Lin, Priya Goyal, Ross Girshick, Kaiming He, and Piotr Dollár. Focal loss for dense object detection. In *Proceedings of the IEEE international conference on computer vision*, pages 2980–2988, 2017. 5
- [44] Ilya Loshchilov and Frank Hutter. Decoupled weight decay regularization. *arXiv preprint arXiv:1711.05101*, 2017. 5
- [45] Yuning Lu, Jianzhuang Liu, Yonggang Zhang, Yajing Liu, and Xinmei Tian. Prompt distribution learning. In *Proceedings of the IEEE/CVF Conference on Computer Vision and Pattern Recognition*, pages 5206–5215, 2022. 3
- [46] Huaishao Luo, Junwei Bao, Youzheng Wu, Xiaodong He, and Tianrui Li. Segclip: Patch aggregation with learnable centers for open-vocabulary semantic segmentation. In *International Conference on Machine Learning*, pages 23033–23044. PMLR, 2023. 2
- [47] M Minderer, A Gritsenko, A Stone, M Neumann, D Weissenborn, A Dosovitskiy, A Mahendran, A Arnab, M Dehghani, Z Shen, et al. Simple open-vocabulary object detection with vision transformers. *arXiv 2022. arXiv preprint arXiv:2205.06230*, 2022. 2
- [48] Giuseppe Pastore, Fabio Cermelli, Yongqin Xian, Massimiliano Mancini, Zeynep Akata, and Barbara Caputo. A closer look at self-training for zero-label semantic segmentation. In *Proceedings of the IEEE/CVF Conference on Computer Vision and Pattern Recognition*, pages 2693–2702, 2021. 6
- [49] Jie Qin, Jie Wu, Pengxiang Yan, Ming Li, Ren Yuxi, Xuefeng Xiao, Yitong Wang, Rui Wang, Shilei Wen, Xin Pan, et al. Freeseg: Unified, universal and open-vocabulary image segmentation. In *Proceedings of the IEEE/CVF Conference on Computer Vision and Pattern Recognition*, pages 19446–19455, 2023. 1, 2
- [50] Alec Radford, Jong Wook Kim, Chris Hallacy, Aditya Ramesh, Gabriel Goh, Sandhini Agarwal, Girish Sastry, Amanda Askell, Pamela Mishkin, Jack Clark, et al. Learning transferable visual models from natural language supervision. In *International conference on machine learning*, pages 8748–8763. PMLR, 2021. 1, 2, 3

- [51] René Ranftl, Alexey Bochkovskiy, and Vladlen Koltun. Vision transformers for dense prediction. In *Proceedings of the IEEE/CVF International Conference on Computer Vision*, pages 12179–12188, 2021. 1, 2
- [52] Yongming Rao, Wenliang Zhao, Guangyi Chen, Yansong Tang, Zheng Zhu, Guan Huang, Jie Zhou, and Jiwen Lu. Densclip: Language-guided dense prediction with context-aware prompting. In *Proceedings of the IEEE/CVF Conference on Computer Vision and Pattern Recognition*, pages 18082–18091, 2022. 1, 3
- [53] Pengzhen Ren, Changlin Li, Hang Xu, Yi Zhu, Guanrun Wang, Jianzhuang Liu, Xiaojun Chang, and Xiaodan Liang. Viewco: Discovering text-supervised segmentation masks via multi-view semantic consistency. *arXiv preprint arXiv:2302.10307*, 2023. 2
- [54] Aurko Roy, Mohammad Saffar, Ashish Vaswani, and David Grangier. Efficient content-based sparse attention with routing transformers. *Transactions of the Association for Computational Linguistics*, 9:53–68, 2021. 5
- [55] Nicholas Roy, Ingmar Posner, Tim Barfoot, Philippe Beaudoin, Yoshua Bengio, Jeannette Bohg, Oliver Brock, Isabelle Depatie, Dieter Fox, Dan Koditschek, et al. From machine learning to robotics: challenges and opportunities for embodied intelligence. *arXiv preprint arXiv:2110.15245*, 2021. 1
- [56] Robin Strudel, Ricardo Garcia, Ivan Laptev, and Cordelia Schmid. Segmenter: Transformer for semantic segmentation. In *Proceedings of the IEEE/CVF international conference on computer vision*, pages 7262–7272, 2021. 1, 2
- [57] Carole H Sudre, Wenqi Li, Tom Vercauteren, Sebastien Ourselin, and M Jorge Cardoso. Generalised dice overlap as a deep learning loss function for highly unbalanced segmentations. In *Deep Learning in Medical Image Analysis and Multimodal Learning for Clinical Decision Support: Third International Workshop, DLMIA 2017, and 7th International Workshop, ML-CDS 2017, Held in Conjunction with MICCAI 2017, Québec City, QC, Canada, September 14, Proceedings 3*, pages 240–248. Springer, 2017. 5
- [58] Ashish Vaswani, Noam Shazeer, Niki Parmar, Jakob Uszkoreit, Llion Jones, Aidan N Gomez, Łukasz Kaiser, and Illia Polosukhin. Attention is all you need. *Advances in neural information processing systems*, 30, 2017. 3
- [59] Yongqin Xian, Subhabrata Choudhury, Yang He, Bernt Schiele, and Zeynep Akata. Semantic projection network for zero-and few-label semantic segmentation. In *Proceedings of the IEEE/CVF Conference on Computer Vision and Pattern Recognition*, pages 8256–8265, 2019. 3, 6
- [60] Hu Xu, Saining Xie, Xiaoqing Ellen Tan, Po-Yao Huang, Russell Howes, Vasu Sharma, Shang-Wen Li, Gargi Ghosh, Luke Zettlemoyer, and Christoph Feichtenhofer. Demystifying clip data. *arXiv preprint arXiv:2309.16671*, 2023. 1, 2
- [61] Jiarui Xu, Shalini De Mello, Sifei Liu, Wonmin Byeon, Thomas Breuel, Jan Kautz, and Xiaolong Wang. Groupvit: Semantic segmentation emerges from text supervision. In *Proceedings of the IEEE/CVF Conference on Computer Vision and Pattern Recognition*, pages 18134–18144, 2022. 2
- [62] Mengde Xu, Zheng Zhang, Fangyun Wei, Yutong Lin, Yue Cao, Han Hu, and Xiang Bai. A simple baseline for open-vocabulary semantic segmentation with pre-trained vision-language model. In *Computer Vision—ECCV 2022: 17th European Conference, Tel Aviv, Israel, October 23–27, 2022, Proceedings, Part XXIX*, pages 736–753. Springer, 2022. 1, 2, 6, 7
- [63] Bowen Zhang, Zhi Tian, Quan Tang, Xiangxiang Chu, Xiaolin Wei, Chunhua Shen, et al. Segvit: Semantic segmentation with plain vision transformers. *Advances in Neural Information Processing Systems*, 35:4971–4982, 2022. 1, 2, 4
- [64] Wenliang Zhao, Yongming Rao, Zuyan Liu, Benlin Liu, Jie Zhou, and Jiwen Lu. Unleashing text-to-image diffusion models for visual perception. *arXiv preprint arXiv:2303.02153*, 2023. 3
- [65] Sixiao Zheng, Jiachen Lu, Hengshuang Zhao, Xiatian Zhu, Zekun Luo, Yabiao Wang, Yanwei Fu, Jianfeng Feng, Tao Xiang, Philip HS Torr, et al. Rethinking semantic segmentation from a sequence-to-sequence perspective with transformers. In *Proceedings of the IEEE/CVF conference on computer vision and pattern recognition*, pages 6881–6890, 2021. 1, 2
- [66] Chong Zhou, Chen Change Loy, and Bo Dai. Extract free dense labels from clip. In *European Conference on Computer Vision (ECCV)*, 2022. 1, 2, 3
- [67] Kaiyang Zhou, Jingkang Yang, Chen Change Loy, and Ziwei Liu. Conditional prompt learning for vision-language models. In *Proceedings of the IEEE/CVF Conference on Computer Vision and Pattern Recognition*, pages 16816–16825, 2022. 3
- [68] Kaiyang Zhou, Jingkang Yang, Chen Change Loy, and Ziwei Liu. Learning to prompt for vision-language models. *International Journal of Computer Vision*, 130(9):2337–2348, 2022. 3
- [69] Ziqin Zhou, Bowen Zhang, Yinjie Lei, Lingqiao Liu, and Yifan Liu. Zegclip: Towards adapting clip for zero-shot semantic segmentation. *arXiv preprint arXiv:2212.03588*, 2022. 1, 2, 3, 4, 5, 6, 7, 8
- [70] Beier Zhu, Yulei Niu, Yucheng Han, Yue Wu, and Hanwang Zhang. Prompt-aligned gradient for prompt tuning. In *Proceedings of the IEEE/CVF International Conference on Computer Vision*, pages 15659–15669, 2023. 3
- [71] Lei Zhu, Xinjiang Wang, Zhanghan Ke, Wayne Zhang, and Rynson Lau. Biformer: Vision transformer with bi-level routing attention. *arXiv preprint arXiv:2303.08810*, 2023. 5